Dalton Transactions

PAPER

Cite this: *Dalton Trans.*, 2015, **44**, 5909

Influence of the ligand frameworks on the coordination environment and properties of new phenylmercury(II) β-oxodithioester complexes†

Gunjan Rajput,[a] Manoj Kumar Yadav,[a] Michael G. B. Drew[b] and Nanhai Singh*[a]

Received 12th December 2014,
Accepted 11th February 2015

DOI: 10.1039/c4dt03816a

www.rsc.org/dalton

New phenylmercury(II) complexes of the form [PhHg(L1), PhHg(L2) and PhHg(L3)] (L1 = methyl-3-hydroxy-3-(*p*-methoxyphenyl)-2-propenedithioate (**1**), L2 = methyl-3-hydroxy-3-(*p*-bromophenyl)-2-propenedithioate (**2**) and L3 = methyl-3-hydroxy-(3-pyridyl)-2-propenedithioate (**3**)) have been synthesized and characterized by elemental analysis, IR, UV-Vis, ^{1}H and ^{13}C NMR. The crystal structures of **1–3** reveal a linear geometry about the mercury atom *via ipso*-C and S11 atoms. **1** and **2** exhibited O,S-coordination whereas **3** preferred S,S-coordination. Intramolecular Hg⋯O bonding interactions are also observed in **1** and **2** at distances of 2.638(14), 2.644(10) Å respectively. However in **3**, incorporation of the 3-pyridyl substituent on the ligand enhanced the proximity of S13 and N14, giving rise to significant intramolecular Hg⋯S and intermolecular Hg⋯N interactions at 3.141(5) Å and 2.77(2) Å respectively generating a 1-D polymeric chain motif. The O,S- or S,S-coordination preference and Hg⋯N interactions have been assessed by DFT calculations. All the complexes show metal perturbed ligand-centred luminescence characteristics in solution and in the solid phase. The band gap values 2.54, 2.66 and 2.61 eV for **1**, **2** and **3**, respectively, evaluated from the diffuse reflectance spectroscopy show the semiconducting nature of the complexes.

Introduction

Metal dithiolato complexes continue to attract the attention of chemists because of their rich structural varieties, electrical conductivity, magnetic and optical properties, single source MOCVD precursors for the preparation of metal sulphides, and wide-ranging industrial applications such as rubber vulcanization accelerators, sensitizers in solar energy schemes, pesticides and fungicides and flotation agents in metallurgy.[1–12] The Hg^{2+} ion with d^{10} configuration shows no stereochemical preferences arising from the ligand field stabilization effects. The majority of neutral homoleptic organomercury(II)/mercury(II) thiolates are two-coordinate linear. However, higher coordination numbers 3, 4, 5 and 6 are also established based on the interplay of bonding interactions between the metal and soft S and hard O or N donor atoms.[13–16] The extremely toxic organomercurials and mercury in other forms are concerned with environmental pollution and serious health hazards. Therefore the coordination chemistry of the mercury(II) ion is of prime importance. The growing interest in the organomercury thiolates is due to detoxification of mercury by metallothionenes (MTs) in DNA binding proteins and in mercuric ion reductase and related proteins.[17–19] Furthermore, the significant luminescence characteristics of Zn^{2+} and Cd^{2+} complexes arising from the metal perturbed intraligand charge transfer transitions are well documented, but studies of the luminescence properties of complexes with the heaviest congener Hg^{2+} are rather limited.[20,21]

Organosulphur compounds including monoanionic β-oxodithioesters and their dithioacid derivatives represent an important class of O,S-donor ligands and are important in metal mediated catalytic processes.[22–24] In spite of the strong affinity of distinctly soft organomercury(II) ion to sulphur donors, to our knowledge details of their dithioester complexes have only recently appeared in the literature.[22c] The hydroxydithio acids (Fig. 1a) and their ester derivatives may exhibit different coordination modes in their complexes

---

[a] *Department of Chemistry, Faculty of Science, Banaras Hindu University, Varanasi 221005, India. Fax: +91-542-2386127; E-mail: nsinghbhu@gmail.com, nsingh@bhu.ac.in*

[b] *Department of Chemistry, University of Reading, Whiteknights, Reading, RG6 6AD, UK*

† Electronic supplementary information (ESI) available: Table S1: simulated and experimental PXRD patterns for **1–3**; Tables S2, S3 and S4: non-conventional hydrogen bonding interactions and their parameters, selected Wiberg bond orders and charge distribution given by NBO analysis for **1** and **3**, respectively; Fig. S5, S6 and S7: solid phase absorption spectra, solution phase excitation and emission spectra, solid phase emission spectra of **1–3**, respectively; Schemes S7 and S8: generalized methodology for the synthesis of ligands and complexes **1–3**, respectively. CCDC 1025406, 1025407 and 925920. For ESI and crystallographic data in CIF or other electronic format see DOI: 10.1039/c4dt03816a

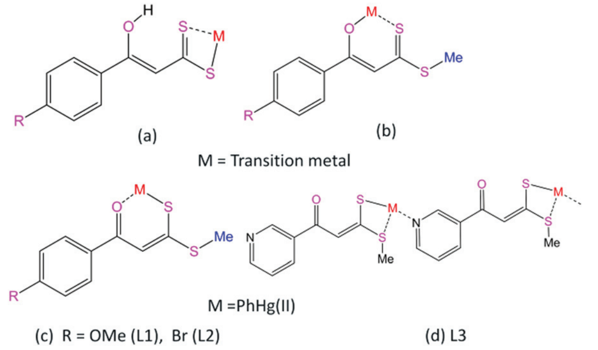

Fig. 1 The coordination modes of (a) hydroxydithio acid and (b–d) their dithioester derivatives.

(Fig. 1). In general, the S,S-coordination mode of the dithio acids forming a four-membered chelate ring dominates over the O,S-coordination with a six-membered chelate ring in the majority of transition metal complexes.[22] However, in transition metal complexes with dithioester derivatives, the O,S-coordination mode (Fig. 1b) is found rather than S,S-coordination because of the weak coordinative ability of the –SMe group. However, it was thought more likely to achieve the S,S-coordination mode with the soft heavy main group metal ions including the mercuric ion.

This was attempted by modifying the dithioester backbone by incorporation of pyridine, –OMe and Br substituents containing hard O and N and soft S and Br donor atoms and preparing their hitherto uninvestigated phenylmercury(II) complexes utilizing dithioesters depicted in Fig. 1c and d. The structural features of the prepared complexes (**1–3**) have been revealed by X-ray crystallography, and their optical (luminescence and diffuse reflectance) and solid phase conducting properties have been studied.

A switch to dithioester ligands with varying substituents may also make significant differences in the structural properties of the complexes. The important reasons for choosing these ligand systems is due to the following facts: (i) the β-oxodithioesters offer both soft and hard donor atoms that may expand their chelating/bridging capabilities; (ii) the different donor atoms on the substituents may facilitate intra- and intermolecular non-covalent/bonding interactions to generate multi-dimensional assemblies of the components; (iii) the extent of S⋯S intermolecular association may affect the conducting properties of the complexes; and (iv) the enhanced conjugation and conformational rigidity provided by the Py(N) may modify the luminescence characteristics of the complexes.

Results and discussion

Synthesis and characterization

Treatment of a methanolic solution of the salts KL1–KL3 with PhHg(OAc) in an equimolar ratio led to the formation of air and moisture stable complexes **1–3** in good yield. The complexes have been characterized by elemental analysis, IR, UV-Vis, ^{1}H and ^{13}C NMR and their structures revealed by X-ray crystallography. The semiconducting behaviour of the complexes has been investigated using diffuse reflectance spectra. The homogeneity of the bulk samples of **1–3** was ascertained by comparing the experimental PXRD patterns with the respective simulated powder patterns obtained from the single crystal data. The experimental and simulated PXRD patterns corroborate well to indicate the phase purity of bulk samples (Fig. S1, ESI†). Their structures revealed attractive intramolecular Hg⋯O bonding interactions in **1** and **2** and intermolecular Hg⋯N interactions in **3**, which have been corroborated by DFT calculations. Their luminescence properties have been studied both in solution and in the solid phase.

Spectroscopy

In the IR spectra, complexes **1–3** show bands at 1604, 1605, 1621; 1588, 1559, 1584 and 1022–1074 cm^{-1} for the $\nu_{\mathrm{C=O}}$, $\nu_{\mathrm{C=C}}$ and $\nu_{\mathrm{C-S}}$ vibrations, respectively, diagnostic of co-ordinated dithioester ligands. The free ligands **HL1–HL3** show characteristic bands at 1179, 1181, 1124; 1603, 1580, 1593 and 1227–1243 cm^{-1} for the $\nu_{\mathrm{C-OH}}$, $\nu_{\mathrm{C=C}}$ and $\nu_{\mathrm{C-S}}$ frequencies, respectively. The decrease in the $\nu_{\mathrm{C-S}}$ frequency in **1–3** in comparison with **HL1–HL3** is indicative of coordination *via* an S atom of the –SCSMe group of the dithioester ligands. The ^{1}H NMR spectra of the ligands **HL1–HL3** show the –OH proton in the δ 14.98–15.17 ppm range, which is absent in complexes **1–3** due to keto–enol tautomerism. The position of the vinylic proton in the free ligands (δ 6.87–6.97 ppm) and complexes (δ 6.83–6.93 ppm) remains almost unchanged. The ^{13}C NMR signal observed at δ 166.11–169.51 ppm for the C–OH carbon in the free ligands is absent in the complexes due to stabilization of the keto form. The vinylic carbon of the ligands showed a chemical shift in the δ 107.08–107.87 ppm range while the corresponding vinylic carbon in the complexes (δ 113.69–114.35 ppm) shows a downfield shift of approximately δ 7 ppm. The –C═S carbon located at δ 215.40–218.32 ppm in the free ligands is observed at δ 137.59–149.06 ppm due to the –C–S carbon in the complexes **1–3**, thereby indicating phenylmercury(II) coordination to sulphur of the –SCSMe group. Accordingly, in the complexes the –C═O carbon is observed at δ 184.66–185.67 ppm. This shows that the keto form of the β-oxodithioester ligands is stabilized in these complexes (crystal structures *vide infra*) instead of the more stable enolate form reported in transition metal complexes.[22]

Crystal structures

Crystallographic details and selected bond distances and bond angles of **1–3** are listed in Tables 1 and 2, respectively. Fig. 2 depicts the ORTEP diagrams of the complexes with displacement ellipsoids at 30% probability.

The structures of **1–3** are essentially based on two-coordinate linear geometry about the Hg atom in which the metal is bonded to the *ipso*-C of the phenyl group at 2.09(2), 2.02(2) and 2.07(2) Å and to S11 from the dithioester at 2.377(4), 2.378(5)

Table 1 Selected bond distances and angles for **1–3**

Bond distances (Å)			
	1	**2**	**3**
Hg1–C41	2.090(19)	2.019(15)	2.072(19)
Hg1–S11	2.377(4)	2.378(5)	2.383(4)
Hg1–S13	—	—	3.141(5)
Hg1–O15/N23$1	2.638(14)	2.644(10)	2.77(2)
S11–C12	1.74(2)	1.71(2)	1.75(2)
S13–C12	1.78(2)	1.78(2)	1.76(2)
C14–C15	1.44(2)	1.48(2)	1.51(2)
C15–O15	1.25(2)	1.23(2)	1.12(2)
C14–C12	1.35(3)	1.36(2)	1.33(2)
Bond angles (°)			
C41–Hg1–S11	176.6(10)	177.9(4)	169.4(5)
Hg1–S11–C12	104.3(7)	105.7(6)	103.5(6)
C12–C14–C15	130(2)	127.6(13)	122.4(15)
C14–C15–O15	122.5(19)	123.1(12)	128.2(15)
C15–O15–Hg1	118.9(13)	119.6(9)	—
S11–Hg1–N23$1	—	—	88.1(3)
S11–Hg1–S13	—	—	62.2(1)
S13–Hg1–C41	—	—	108.7(5)
C41–Hg1–N23$1	—	—	102.3(6)

Symmetry element $1 1 + x, y, 1 + z.

Table 2 Crystal refinement parameters

Compound	**1**	**2**	**3**
Chemical formula	$C_{17}H_{16}HgO_2S_2$	$C_{16}H_{13}BrHgOS_2$	$C_{15}H_{13}HgNOS_2$
Formula weight	517.01	565.88	487.97
Crystal system	Monoclinic	Monoclinic	Monoclinic
Space group	$P2_1$	$P2_1/c$	Cc
a (Å)	11.7409(15)	14.070(2)	8.4810(5)
b (Å)	5.3998(10)	5.2265(6)	21.8202(12)
c (Å)	13.192(2)	23.417(3)	8.5851(3)
β (°)	93.737(14)	107.24(2)	104.740(4)
V (Å^3)	834.6(2)	1644.6(4)	1536.45(14)
Z	2	4	4
ρ_{calc} (g cm^{-3})	2.057	2.289	2.110
T (K)	293(2)	293(2)	293(2)
μ (Mo Kα) (mm^{-1})	9.474	12.053	10.283
F(000)	492	1056	920
Reflections collected	3457	7973	3829
Independent reflns	2912	2750	2999
Reflections with $I > 2\sigma(I)$	2050	2110	2500
Final indices [$I > 2\sigma(I)$] R_1 [a], wR_2 [b]	0.072, 0.160	0.064, 0.168	0.055, 0.145
$R_{1[a]}$, w$R_{2[b]}$ [all data]	0.102, 0.173	0.085, 0.189	0.070, 0.157
Flack constant	0.00(3)	n/a	0.00(2)
GOF	0.958	0.993	1.073
Max., min. residual electron density (e Å^{-3})	2.33, −1.76	2.36, −1.64	2.50, −1.55

[a] $R_1 = \sum||F_o| - |F_c||/\sum|F_o|$. [b] $R_2 = \{[\sum w(F_o^2 - F_c^2)/\sum w(F_o^2)^2]\}^{1/2}$, $w = 1/[\sigma^2(F_o^2) + (xP)^2]$, where $P = (F_o^2 + 2F_c^2)/3$.

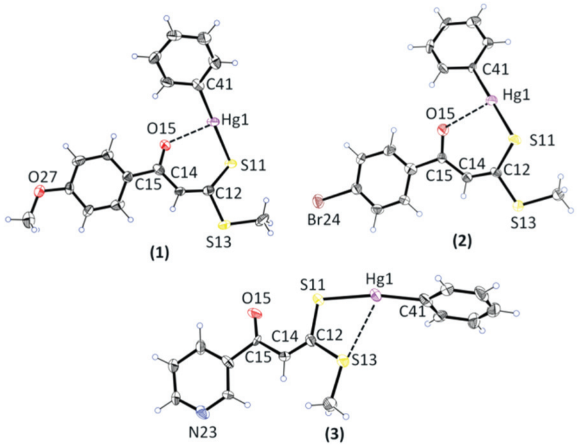

Fig. 2 ORTEP representations of **1–3** with displacement ellipsoids at 30% probability. Dotted lines represent weak interactions.

and 2.383(4) Å in **1**, **2** and **3**, respectively. The Hg1⋯O15 distances of 2.638(14) and 2.644(10) Å in **1** and **2** and the Hg1⋯S13 distance of 3.141(5) Å in **3** are indicative of secondary bonding interactions in these three complexes. The C41–Hg1–S11 angles of 176.6(10), 177.9(4) and 169.4(5)° in **1**, **2** and **3**, respectively, show significant deviations from linearity, more pronounced in **3** owing to significant interactions between soft Hg and hard N atoms from the neighbouring molecule. The C12–C14 double bond lengths for **1–3** at 1.35(2), 1.36(3) and 1.33(3) Å respectively show distinct double bond character.

It has to be noted that the C15–O15 carbonyl bond lengths of (1.25(2), 1.23(2) Å) in (**1**, **2**) are consistent with these being partial double bonds. The C12–S11 distances of 1.74(2) and 1.71(2) Å and the slightly longer C12–S13 distances of 1.78(2) and 1.78(2) Å are in the range of the C–S single bond lengths. These observations point towards some delocalization of electron density over the six-membered chelate ring composed of O15, C15, C14, C12, S11 and Hg1 atoms in these complexes (Fig. 2). By comparison, the C15–O15 distance in **3** at 1.12(2) Å corresponds to C–O double bond length and is significantly shorter than those observed in **1** and **2**. Notably, in **3** the C12–S11 and C12–S13 bond lengths at 1.75(2) and 1.76(2) are consistent with both sulphur atoms being bonded to the metal, and are considerably shorter than the C–S single bond (*ca.* 1.81 Å), a fact which can be related to π-delocalization over the CS_2 unit forming a four-membered chelate ring defined by S11, C12, S13 and Hg1 atoms in the polymeric structure (Fig. 2 and 3c). These metric parameters indicate that the stronger thiophilicity of phenylmercury(II) led to coordination through S11 of the –SCSMe group of the dithioester ligands in **1–3**. More interestingly, the S,S-coordination in **3** is stabilized as opposed to the O,S-coordination generally found in their transition metal complexes.[22] The crystal structures of these complexes provide evidence for participation of the β-keto form of dithioesters which to our knowledge has not been previously established by spectroscopic and crystallographic studies but is known to exist in solution.[23a]

In (**1**, **2**) the carbonyl oxygen of the ligands lies close to the Hg atom (Fig. 2) with Hg⋯O distances at 2.638(14) and 2.644(10)

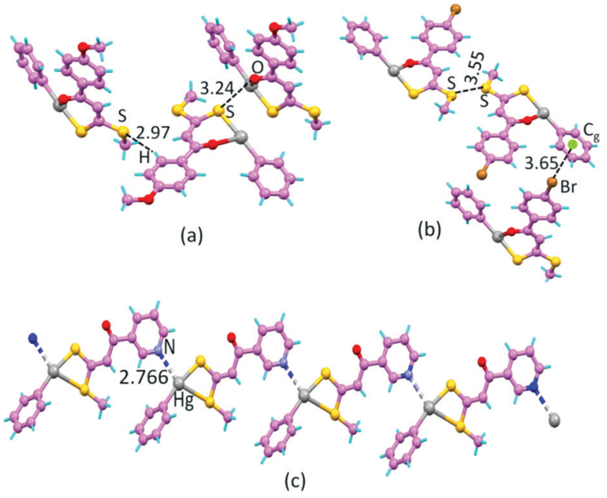

Fig. 3 (a) Weak intermolecular O⋯S and S⋯H interactions in **1**; (b) S⋯S and Br⋯π interactions in **2**; (c) intermolecular Hg⋯N bonding interactions in **3** giving rise to a 1-D polymeric chain. Distances are reported in Å.

Å significantly smaller than the sum of van der Waals radii[25] of 3.23 Å. This weaker bond augments the strong linear geometry to establish a distorted T-shaped structure about the Hg atom with C41–Hg1–O15, S11–Hg1–O15 and C41–Hg1–S11 angles, respectively, at 102.0(9), 79.3(9) and 176.6(10)° for **1** and 99.4(5), 79.5(3) and 177.9(4)° for **2**. While in **3**, the N atom of the pyridine on each molecule is directed towards the mercury centre on the adjacent molecule to form intermolecular Hg⋯N contacts[14a–e,16a] (1 + *x*, *y*, 1 + *z*) at a somewhat longer distance of 2.77(2) Å. These Hg–N contacts are comparable to intramolecular Hg–N contacts found in previous structures.[14f–h] Thus, the crystal structure of **3** forms a 1-D polymeric chain structure (Fig. 3c) and, overall, a four coordinate distorted tetrahedral geometry is established about the Hg atom. The value of τ_4 for four coordinate complexes[26] ranges between 0 for square planar[15] and 1 for tetrahedral and is found to be 0.58 for **3** which is intermediate between the two geometries but slightly more distorted towards the tetrahedral geometry. The presence of hard donor atoms in the vicinity and structural rigidity can be attributed to these hard–soft bonding/interactions in the complexes.

The significant changes in the bonding patterns about the PhHg(II) ion in **1**–**3** are worth noting. In **1** and **2** the intramolecular Hg⋯O bonding interactions are preferred over the soft Hg⋯S (of –SMe group) bonding because of the low coordinative ability of the –SMe group. These bonding preferences have been assessed by DFT calculations (*vide infra*). The crystal structures of **1**–**3** are stabilized by weak C–H⋯S, C–H⋯O, Br⋯π and S⋯S interactions (Fig. 3; Table S2, ESI†). In **2**, the S13⋯S13 (1 − *x*, −*y*, 1 − *z*) interactions are at a distance of 3.544(4) Å (Fig. 3b); the closest Hg–Hg distances[25] in **1** and **2** are at 4.389(1) and 4.367(1) Å, far longer than the sum of van der Waals radii, *i.e.* 3.46 Å, while in **3** the Hg atoms are further apart at 5.263(1) Å.

Theoretical calculations

The preference of O,S-coordination in **1** and **2** and S,S in **3** was assessed by some DFT calculations of the structure in **1** and an alternate simulated structure in which the two sulphur atoms were bonded to the metal as in **3**. After geometry optimisation, the structure **1** with Hg⋯O bonding was preferred by an energy of 9.88 kcal mol^{-1}. These calculations were then repeated with a pyridine ligand added and the (O,S) chelate was favoured over the (S,S) chelate by 8.00 kcal mol^{-1}. This implies that the (S,S) chelate structure found in **3** is primarily the result of packing effects which overcome the greater preference for (O,S) chelation.

In **3**, the role of Hg⋯N bonding interactions was examined by using the model shown in Fig. 4b but having three adjacent molecules linked by Hg⋯N contacts. Single point calculations showed that the ground state energy difference between a molecule of **3** and a trimeric model (*i.e.* $E_{\text{trimer}} - \mathbf{3}E_{\text{monomer}}$) is −15.29 kcal mol^{-1}, thus showing the extra stability generated by forming the 1-D polymeric chain motif in **3**.

Wiberg bond indices by NBO analysis were calculated based on the geometry optimized structures of **1** (Fig. 2) and **3** (Fig. 4b) and the results are shown in Tables S3 and S4, ESI.† In the optimized structure of **1** the calculated Hg⋯O distance is at 2.42 Å, much shorter than the experimental distance, while the Hg1–S11 bond at 2.60 Å is slightly longer than the experimental value. This suggests that the absence of the Hg⋯N contact in the monomer is compensated for by the strengthening of the Hg⋯O bonding interactions, and conversely the presence of the Hg⋯N contact in the 1-D polymer in the solid state weakens the Hg⋯O interactions. By contrast, in the dimeric model of **3**, the Hg⋯N contacts were calculated at 2.75 Å, which is the same as that found experimentally (2.76 Å) and the Hg1–S11 bond at a longer distance of 2.56 Å. The Wiberg bond index of 0.117 indicates weak Hg⋯O bonding in **1** whereas in the case of Hg⋯N contacts in **3** the value is 0.093, which denotes Coulombic interaction only, rather than a chemical interaction.

The NBO charge analysis shows a negative charge of −0.718 and −0.511 on O(15) and N(23) atoms in **1** and the dimer of **3**, respectively, whereas the metal centre possesses a positive charge of approximately 1.0 in both the complexes. In **1**, the *E*(2) values for the most significant stabilization energies are

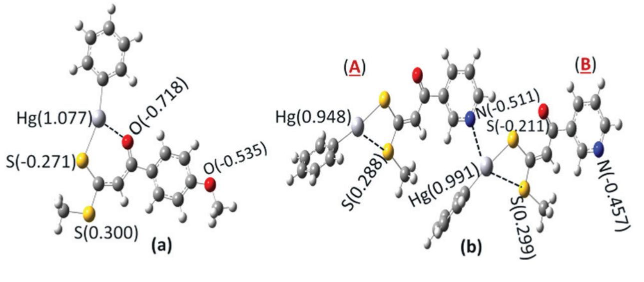

Fig. 4 Optimized geometries and selected charge parameters (in parentheses) calculated from an NBO analysis for (a) **1** and (b) **3**; (A) and (B) denote each fragment of the dimer.

seen at 1.38 kcal mol^{-1} for donor interaction between bonding O–C (BD, NBO 7) and metal centred empty orbitals (LP*, NBO 92) and at 14.90 kcal mol^{-1} which is the sum of stabilization energies due to donor interaction between the O lone pair (LP(1), NBO 76; LP(2), NBO 77) and metal centred empty orbitals (LP*, NBO 92). In **3**, the large $E(2)$ value at 11.84 kcal mol^{-1} shows strong stabilization for donor interaction between the N lone pair (LP, NBO152) and metal centred empty orbitals (LP*, NBO 159).

Optical properties

Absorption and emission. The absorption spectra of complexes **1–3** were recorded in a dichloromethane solution (Fig. 5) and in the solid as Nujol mull (Fig. S5, ESI†). They show almost similar absorption features apart from variations in the peak intensity. The bands near 250 nm (ε = 1.61–2.23 × 10^4 M^{-1} cm^{-1}), 300 nm (ε = 9.4 × 10^3–1.29 × 10^4 M^{-1} cm^{-1}) and 350 nm (ε = 1.60–2.08 × 10^4 M^{-1} cm^{-1}) are assigned to metal perturbed ligand centered intraligand charge transfer (ILCT) transitions.[14a–e,16a] In the case of **1** an additional intense absorption is also observed at 400 nm (ε = 2.07 × 10^4 M^{-1} cm^{-1}).

When excited at 340 nm in CH_2Cl_2 solution, complexes **1–3** show unstructured strong broad emission bands with λ_{emis}^{max} at 420 nm (Fig. S6, ESI†) that emanates from the metal perturbed ILCT state. Upon excitation at 350 nm in the solid phase, **1–3** exhibit λ_{emis}^{max} at 480 nm at room temperature with a noticeable red shift in comparison with their solution spectra (Fig. S7, ESI†). This indicates that the luminescent chromophore is only slightly altered in the two media. The excitation spectra for the complexes in solution show that λ_{emis}^{max} at 340 nm almost matches their UV-Vis spectra (Fig. 5). The unusual luminescence properties of the mercury(II) complexes have been ascribed to prominent metallophilic interactions in the past.[20,21] The somewhat higher red shifted Stokes shifts of about 50 nm in the solid phase as compared to the solution spectra can be associated with the presence of weak Hg⋯Hg interactions[20] (*vide supra* in the crystal structure) in (**1**, **2**) and the conformational rigidity and enhanced conjugation due to the Py(N) lone pair of electrons in the extended structure in **3**. This clearly reveals the relationship between structure and luminescence properties of the complexes.

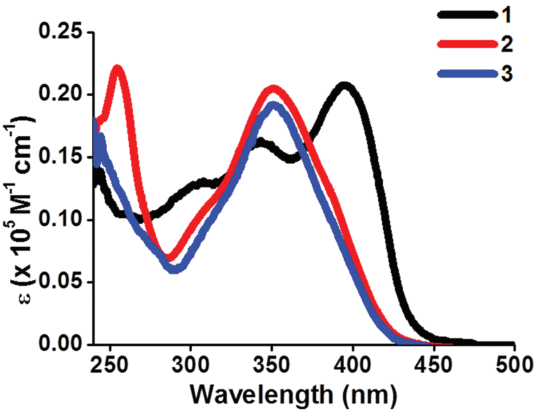

Fig. 5 Absorption spectra of complexes **1–3** in dichloromethane.

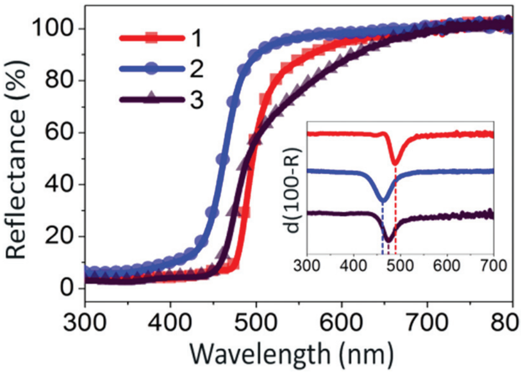

Fig. 6 Diffuse reflectance spectra of **1–3** along with the first differential shown in the inset.

Diffuse reflectance spectra

The diffuse reflectance spectra were recorded against $BaSO_4$ as a standard at ambient temperature to evaluate the band gap for **1–3** (Fig. 6). The band gaps (E_g/eV) for **1–3** were found to be 2.54, 2.66 and 2.61, respectively, and were calculated according to the Planck relationship, *i.e.*, $E_g = h\nu = hc/\lambda$, where h is the Planck's constant (4.1357 × 10^{-15} eV s), c is the velocity of light (2.998 × 10^8 m s^{-1}) and λ is the wavelength (nm). The suitable wavelength for band gap determination was ascertained by the first differential of diffuse reflectance spectra and was found to be 489, 462 and 475 nm for **1–3**, respectively, as presented in the inset of Fig. 6. These calculated band gap values are consistent with the semiconducting nature of the complexes.[27]

Experimental section

The experimental details pertaining to elemental analyses (C, H, N) and recording of IR (KBr), ^1H and $^{13}C\{^1H\}$ NMR and UV-Vis spectra are the same as those described elsewhere.[14a–e] X-ray powder diffraction data were collected using a Rigaku MultiFlex-600 system with Cu-K_α radiation. The photoluminescence characteristics in CH_2Cl_2 solution and in the solid state were measured at room temperature using a Fluorolog Horiba Jobin Yvon spectrophotometer. Diffuse reflectance spectra were recorded on a Harrick Praying Mantis accessory on a Shimadzu UV-3600 spectrophotometer. All the chemicals used were of reagent grade and were obtained from the commercial sources.

General procedures

Synthesis of ligands HL1–HL3. The ligands methyl-3-hydroxy-3-(*p*-methoxyphenyl)-2-propenedithioate **HL1**, methyl-3-hydroxy-3-(*p*-bromophenyl)-2-propenedithioate **HL2** and methyl-3-hydroxy-(3-pyridyl)-2-propenedithioate **HL3** were synthesized by the following procedure. To a solution of sodium hydride (0.6 g, 25 mmol) dissolved in a DMF : hexane mixture

(4 : 1; 20 mL) were added dropwise 4-methoxyacetophenone (1.5 g, 10.0 mmol) (for H**L1**), 4-bromoacetophenone (2.0 g, 10.0 mmol) (for H**L2**), 3-acetylpyridine (1.21 g, 10.0 mmol) (for H**L3**) in DMF (20 mL). After stirring for 1 h in an ice bath under an N_2 atmosphere, a solution of the dimethyltrithiocarbonate (TTC)[28] (1 mL, 4.48 mmol) was added and the mixture was stirred at room temperature for another 8 h (Scheme S8, ESI†). Excess NaH was neutralized by adding 0.1 M HCl (50 mL), and the product was extracted with three 50 mL portions of ethyl acetate, washed with brine solution and water, dried over $MgSO_4$, and concentrated. The product was purified by silica gel (100–200 mesh) chromatography using hexane as the eluent to obtain a crystalline yellow solid.

[H**L1**] Yield: (0.197 g, 82%). Anal. Calcd for: $C_{11}H_{12}O_2S_2$ (240.34): C 54.97, H 5.03%. Found: C 54.74, H 5.09%. IR (KBr, cm^{-1}): ν = 1179 (ν_{C-OH}), 1603 ($\nu_{C=C}$), 1231 ($\nu_{C=S}$). ^1H NMR (300.40 MHz, $CDCl_3$): δ 15.17 (s, 1H, –C(OH)–), 7.86 (d, 2H, C_6H_4, J = 9.01 Hz), 6.95 (d, 2H, C_6H_4, J = 9.01 Hz), 6.97 (s, 1H, –CH=C–), 3.86 (s, 3H, –OCH_3), 2.64(s, 3H, –SCH_3) ppm. ^{13}C NMR (74.45 MHz, $CDCl_3$): δ 16.96 (–SCH_3), 55.51 (–OCH_3), 107.08 (–CH=C–), 162.81, 128.68, 126.21, 114.40 (C_6H_4), 169.51 (–C(OH)–), 215.62 (–C=S) ppm.

[H**L2**] Yield: (0.252 g, 87%). Anal. Calcd for: $C_{10}H_9BrOS_2$ (289.21): C 41.53, H 3.14%. Found: C 41.38, H 3.22%. IR (KBr, cm^{-1}): ν = 1181 (ν_{C-OH}), 1580 ($\nu_{C=C}$), 1243 ($\nu_{C=S}$). ^1H NMR ($CDCl_3$): δ 14.99 (s, 1H, –C(OH)–), 7.80 (d, 2H, C_6H_4, J = 9.01 Hz), 7.63 (d, 2H, C_6H_4, J = 9.01 Hz), 6.87 (s, 1H, –CH=C–), 2.70 (s, 3H, –SCH_3) ppm. ^{13}C NMR (75.45 MHz, $CDCl_3$): δ 17.20 (–SCH_3), 107.87 (–CH=C–), 136.39, 134.58, 129.63, 122.95 (C_6H_4), 167.09 (–C(OH)–), 216.62 (–C=S) ppm.

[H**L3**] Yield: (0.144 g, 68%). Anal. Calcd for: $C_9H_9NOS_2$ (211.30) C 51.16, H 4.29, N 6.63%. Found: C 51.06, H 4.36, N 6.73%. IR (KBr, cm^{-1}): ν = 1124 (ν_{C-OH}), 1593 ($\nu_{C=C}$), 1227 ($\nu_{C=S}$). ^1H NMR (300.70 MHz, $CDCl_3$): δ 14.98 (s, 1H, –C(OH)–), 9.08, 8.71, 8.15, 7.41 (m, 4H, C_5H_4N), 6.91(s, 1H, –CH=C–), 2.75 (s, 3H, –SCH_3) ppm. ^{13}C NMR (74.45 MHz, $CDCl_3$): δ 17.30 (–SCH_3), 107.87 (–CH=C), 152.03, 147.84, 133.96, 130.25, 123.44 (C_5H_4N), 166.11 (–C(OH)–), 218.32 (–C=S) ppm.

Synthesis of complexes 1–3. To a stirring 10 mL acetone solution of the ligand H**L1** (0.240 g, 1 mmol), H**L2** (0.290 g, 1 mmol), or H**L3** (0.211 g, 1 mmol) was added solid K_2CO_3 (0.207 g, 1.5 mmol) separately and in each case the reaction mixture was additionally stirred for 4 h under reflux conditions. The solution was cooled, filtered and dried on a vacuum evaporator to yield the potassium salt of the ligands KL1, KL2 and KL3 as yellow to orange solid products. To a 10 mL stirring aqueous methanolic solution of KL1–KL3 was added a suspension of $PhHg(CO_2CH_3)$ (0.336 g, 1 mmol) in 10 mL methanol and further stirred for 1 h (Scheme S9, ESI†). The yellow solid thus formed was filtered off, washed with methanol, dried in the open and dissolved in dichloromethane to yield yellow crystals within 3–4 weeks.

[PhHg(L1)] (**1**): Yield: (0.440 g, 85%). M.pt. 135–137 °C. Anal. Calcd for $C_{17}H_{16}HgO_2S_2$ (517.01): C 39.49, H 3.12%. Found: C 39.28, H 3.15%. IR (KBr, cm^{-1}): 1604 ($\nu_{C=O}$), 1588 ($\nu_{C=C}$). ^1H NMR (300.40 MHz, $CDCl_3$, ppm): δ 2.51 (s, 3H, –SCH_3), 3.78 (s, 3H, –OCH_3), 6.83 (1H, s,–CH=C–), 6.86–7.86 (m, 9H, Ar–H). ^{13}C {^1H} NMR (75.45 MHz, $CDCl_3$, ppm) δ 18.74 (–SCH_3), 55.41 (–OCH_3), 113.69 (–CH=C–), 128.29–136.46 (Ar–C), 137.59 (=C–S–), 185.67 (–C=O). UV-Vis. (CH_2Cl_2, λ_{max} (nm), ε (M^{-1} cm^{-1})): 244 (1.35×10^4), 304 (1.29×10^4), 345 (1.60×10^4), 394 (2.07×10^4); (Nujol, λ_{max} (nm)): 320, 340 and 424.

[PhHg(L2)] (**2**): Yield: (0.464 g, 82%). M.pt. 136–138 °C. Anal. Calcd for $C_{16}H_{13}BrHgOS_2$ (565.88): C 33.96, H 2.32%. Found: C 33.79, H 2.43%. IR (KBr, cm^{-1}): 1605 ($\nu_{C=O}$), 1559 ($\nu_{C=C}$). ^1H NMR (300.40 MHz, $CDCl_3$, ppm): δ 2.64 (s, 3H, –SCH_3), 6.93 (^1H, s, –CH=C–), 6.93–8.02 (m, 9H, Ar–H). ^{13}C{^1H} NMR (75.45 MHz, $CDCl_3$, ppm) δ 18.82 (–SCH_3), 114.35 (–CH=C–), 122.82–136.50 (Ar–C), 141.98 (=C–S–), 185.18 (–C=O). UV-Vis. (CH_2Cl_2, λ_{max} (nm), ε (M^{-1} cm^{-1})): 253 (2.23×10^4), 304 (1.03×10^4), 350 (2.08×10^4); (Nujol, λ_{max} (nm)): 326, 363 and 418.

[PhHg(L3)] (**3**): Yield: (0.400 g, 80%). M.pt. 142–144 °C. Anal. Calcd for $C_{15}H_{13}HgNOS_2$ (487.97): C 36.92, H 2.69, N 2.87%. Found: C 36.70, H 2.82, N 3.03%. IR (KBr, cm^{-1}): 1621 ($\nu_{C=O}$), 1584 ($\nu_{C=C}$). ^1H NMR (300.40 MHz, $CDCl_3$, ppm): δ 2.62 (s, 3H, –SCH_3), 6.93 (1H, s, –CH=C–), 7.25–7.42 (m, 6H, Ar–H), 8.20, 8.72, 9.11 (m, 3H, C_5H_4N). ^{13}C{^1H} NMR (75.45 MHz, $CDCl_3$, ppm) δ 18.88 (–S–CH_3), 114.04 (–CH=C–), 128.33–137.60 (Ar–C), 149.06 (=C–S–), 152.41, 156.98 (C_5H_4N), 184.66 (–C=O). UV-Vis. (CH_2Cl_2, λ_{max} (nm), ε (M^{-1} cm^{-1})): 245 (1.61×10^4), 310 (9.4×10^3), 350 (1.92×10^4); (Nujol, λ_{max} (nm)): 325, 365 and 436.

X-ray crystal structure determination

Single crystals of **1–3** were obtained by slow evaporation of solutions of the compound in CH_2Cl_2. Single crystal X-ray diffraction data were collected on an Oxford X-calibur CCD diffractometer at 293 K using Mo Kα radiation. Data reduction was carried out using the CrysAlis program.[29] The structures were solved by direct methods using SHELXS-97[30] and refined on F^2 by full matrix least-squares method using SHELXL-97.[31] Non-hydrogen atoms were refined anisotropically and hydrogen atoms were geometrically fixed with thermal parameters equivalent to 1.2 times that of the atom to which they were bonded. Diagrams for the complexes were prepared using ORTEP,[32] Mercury[33] and GaussView[34] software. Crystal data for **1**, **2** and **3** have been deposited at the Cambridge Crystallographic Data Centre with reference numbers CCDC 1025406, 1025407, and 925920.

Computational details

All calculations were carried out using the Gaussian 09 program.[35] Calculations were carried out using the B3LYP density functional together with the basis sets LANL2DZ for metal, 6-31+G* for S, O and N and 6-31G for the remaining atoms. Starting models were taken from the crystal structures but with hydrogen atoms given theoretical positions. Computed interaction energies were corrected for BSSE using the Boys–Bernardi counterpoise correction scheme. The natural atomic charges and Wiberg bond indices were calculated using the natural bond orbital analysis implemented in G09.

Conclusions

The crystal structures of **1**–**3** reveal linear geometry about the mercury atom *via ipso*-C and sulphur atoms. Intramolecular Hg⋯O bonding interactions are observed in **1** and **2**. However, in **3**, incorporation of the 3-pyridyl substituent on the ligand gave rise to (S,S) chelation on the metal together with intermolecular Hg⋯N interactions generating a 1-D polymeric chain motif. These interactions have been assessed by DFT calculations. **1** and **2** show O,S-coordination while S,S-coordination is observed in **3**. To our knowledge, this is the first time that S,S-coordination has been observed with β-oxodithioester ligands and is more likely due to packing effects brought about by the presence of the N-bonding interactions. These complexes strongly luminesce in solution and in the solid phase, which originate from the metal perturbed intra ligand charge transfer transitions. The somewhat more red shifted emissions in the solid phase are attributed to the weaker Hg⋯Hg interactions (**1**, **2**) and the increased conjugation due to the pyridine lone pair in the extended delocalized structure in **3**. The band gap values suggest the semiconducting nature of the complexes. This study demonstrates that the mercury(II) and other heavy main group metal complexes of functionalized β-oxodithioesters may be useful for the design of new compounds with promising material properties.

Acknowledgements

Financial support from the Council of Scientific and Industrial Research (CSIR), New Delhi, project no. 01 (2679)/12/EMR-II (NS, MKY) and SRF (GR), is gratefully acknowledged and the Department of Chemistry, CAS-UGC-I, Banaras Hindu University for the X-ray facilities.

Notes and references

1 (*a*) D. Coucouvanis, *Prog. Inorg. Chem.*, 1970, **11**, 233; (*b*) D. Coucouvanis, *Prog. Inorg. Chem.*, 1979, **26**, 301.

2 (*a*) G. Hogarth, *Prog. Inorg. Chem.*, 2005, **53**, 71; (*b*) S. Naeem, S. A. Serapian, A. Toscani, A. J. P. White, G. Hogarth and J. D. E. T. Wilton-Ely, *Inorg. Chem.*, 2014, **53**, 2404.

3 (*a*) J. Cookson and P. D. Beer, *Dalton Trans.*, 2007, 1459; (*b*) S. Naeem, L. Delaude, A. J. P. White and J. D. E. T. Wilton-Ely, *Inorg. Chem.*, 2010, **49**, 1784.

4 (*a*) E. R. T. Tiekink and I. Haiduc, *Prog. Inorg. Chem.*, 2005, **54**, 127; (*b*) C. S. Lai and E. R. T. Tiekink, *CrystEngComm*, 2003, **5**, 253.

5 P. J. Heard, *Prog. Inorg. Chem.*, 2005, **53**, 268.

6 (*a*) I. Haiduc, in *Handbook of Chalcogen Chemistry*, ed. F. Devillanova, Royal Society of Chemistry, Cambridge, 2007, p. 593; (*b*) I. Haiduc, Secondary Bonding, in *Encyclopaedia of Supramolecular Chemistry*, ed. J. L. Atwood and J. W. Steed, M. Dekker, New York, 2004, p. 1215.

7 P. Cassoux and L. Valade, *Inorganic Materials*, John Wiley and Sons, Chichester, 1996.

8 A. T. Coomber, D. Beljonne, R. H. Friend, J. L. Bredas, A. Charlton, N. Robertson, A. E. Underhill, M. Kurmoo and P. Day, *Nature*, 1996, **380**, 144.

9 T. Okubo, H. Anma, N. Tanaka, K. Himoto, S. Seki, A. Seki, M. Maekaw and T. K-Sowa, *Chem. Commun.*, 2013, **49**, 4316.

10 (*a*) P. O'Brien, J. H. Park and J. Waters, *Thin Solid Films*, 2003, **431**, 502; (*b*) Y. S. Tan, A. L. Sudlow, K. C. Molloy, Y. Morishima, K. Fujisawa, W. J. Jackson, W. Henderson, S. N. B. A. Halim, S. W. Neg and E. R. T. Tiekink, *Cryst. Growth Des.*, 2013, **13**, 3046.

11 A. A. Abramov and K. S. E. Forssberg, *Miner. Process. Extr. Metall. Rev.*, 2005, **26**, 77.

12 (*a*) H. Alper, F. W. B. Einstein, F. W. Hartstock and A. C. Willis, *J. Am. Chem. Soc.*, 1985, **107**, 173; (*b*) L. F. Lindoy, *Coord. Chem. Rev.*, 1969, **4**, 41.

13 (*a*) S. J. Sabounchei, H. Nemattalab, S. Salehzadeh, M. Bayat, H. R. Khavasi and H. Adams, *J. Organomet. Chem.*, 2008, **693**, 1975; (*b*) L. K. Li, Y. L. Song, H. W. Hou, Z. S. Liu, Y. T. Fan and Y. Zhu, *Inorg. Chim. Acta*, 2005, **358**, 3259; (*c*) M. M. Ebrahim, E. H. Stoeckli and K. Panchanatheswaran, *Polyhedron*, 2007, **26**, 3491; (*d*) T. J. Burchell, D. J. Eisler and R. J. Puddephatt, *Inorg. Chem.*, 2004, **43**, 5550; (*e*) H. J. Nam, H. J. Lee and D. Y. Noh, *Polyhedron*, 2004, **23**, 115.

14 (*a*) G. Rajput, M. K. Yadav, T. S. Thakur, M. G. B. Drew and N. Singh, *Polyhedron*, 2014, **69**, 225; (*b*) V. Singh, V. Kumar, A. N. Gupta, M. G. B. Drew and N. Singh, *New J. Chem.*, 2014, **38**, 3737; (*c*) V. Singh, A. Kumar, R. Prasad, G. Rajput, M. G. B. Drew and N. Singh, *CrystEngComm*, 2011, **13**, 6817; (*d*) N. Singh, A. Kumar, R. Prasad, K. C. Molloy and M. F. Mahon, *Dalton Trans.*, 2010, **39**, 2667; (*e*) N. Singh, A. Kumar, K. C. Molloy and M. F. Mahon, *Dalton Trans.*, 2008, 4999; (*f*) S. R. Tamang, J.-H. Son and J. D. Hoefelmeyer, *Dalton Trans.*, 2014, **43**, 7139; (*g*) K. G. von Eschwege, F. Mullera and A. Muller, *Acta Crystallogr., Sect. E: Struct. Rep. Online*, 2011, **67**, m1858; (*h*) A. Castifieiras, W. Hiller, J. Strahle, J. Bravo, J. S. Casas, M. Gayoso and J. Sordo, *J. Chem. Soc., Dalton Trans.*, 1986, 1945.

15 (*a*) H. R. Khavasi and B. M. M. Sadegh, *Dalton Trans.*, 2014, **43**, 5564; (*b*) R. Haid, R. Gutmann, G. Czermak, C. Langes, W. Oberhauser, H. Kopacka, K.-H. Ongania and P. Bruggeller, *Inorg. Chem. Commun.*, 2003, **6**, 61; (*c*) Y. Cbeng, T. J. Emge and J. G. Brennan, *Inorg. Chem.*, 1994, **33**, 3711; (*d*) C. O. Kienitz, C. Tho1ne and P. G. Jones, *Inorg. Chem.*, 1996, **35**, 3990; (*e*) P. C. Healy and A. H. White, *J. Chem. Soc., Dalton Trans.*, 1973, 284.

16 (*a*) X.-Y. Tang, R.-X. Yuan, Z.-G. Ren, H.-X. Li, Y. Zhang and J.-P. Lang, *Inorg. Chem.*, 2009, **48**, 2639; (*b*) T. J. Taylor, C. N. Burress and F. P. Gabbai, *Organometallics*, 2007, **26**, 5252; (*c*) M. Kato, K. Kojima, T. Okamura, H. Yamamoto,

T. Yamamura and N. Ueyama, *Inorg. Chem.*, 2005, **44**, 4037; (*d*) H. Fleischer, Y. Dienes, B. Mathiasch, V. Schmitt and D. Schollmeyer, *Inorg. Chem.*, 2005, **44**, 8087; (*e*) C. M. V. Stalhandske, C. I. Stalhandske, M. Sandsrom and I. Persson, *Inorg. Chem.*, 1997, **36**, 3167.

17 (*a*) A. Sigel and H. Sigel, Metal Ions, in *Biological Chemical Toxicology and Clinical Chemistry of Metals*, ed. S. S. Brown and J. Savoy, Dekker, New York, 1997.

18 *Metallothioneins: Synthesis, Structure and Properties of Metallothioneins, Phytochelatins and Metal-Thiolate Complexes*, ed. M. J. Stillman, C. F. Shaw and K. T. Suzuki, John Wiley & Sons, New York, 1992.

19 G. Henkel and B. Kreb, *Chem. Rev.*, 2004, **104**, 801.

20 (*a*) J. B. King, M. R. Haneline, M. Tsunoda and F. P. Gabbai, *J. Am. Chem. Soc.*, 2002, **124**, 9350; (*b*) M. R. Haneline, M. Tsunoda and F. P. Gabbaï, *J. Am. Chem. Soc.*, 2002, **124**, 3737.

21 (*a*) P. Pyykkö, *Chem. Rev.*, 1997, **97**, 597; (*b*) P. Pyykkö and M. Straka, *Phys. Chem. Chem. Phys.*, 2000, **2**, 2489.

22 (*a*) R. Saumweber, C. Robl and W. Weigand, *Inorg. Chim. Acta*, 1998, **269**, 83; (*b*) I. G-Orozco, M. C. O-Alfaro, J. G. L-Cortes, R. A. Toscano and C. A-Toledano, *Inorg. Chem.*, 2006, **45**, 1766; (*c*) B. N. Ahamed, M. Arunachalam and P. Ghosh, *Inorg. Chem.*, 2010, **49**, 4447; (*d*) I. G-Orozco, J. G. L-Corte's, M. C. O-Alfaro, R. A. Toscano, G. P-Carrillo and C. A-Toledano, *Inorg. Chem.*, 2004, **43**, 8572.

23 (*a*) S. Chowdhury, T. Chanda, A. Gupta, S. Koley, B. J. Ramulu, R. C. F. Jones and M. S. Singh, *Eur. J. Org. Chem.*, 2014, 2964; (*b*) O. M. Singh and N. S. Devi, *J. Org. Chem.*, 2009, **74**, 3141; (*c*) B. S. Mandimutsira, J. L. Yamarik, T. C. Brunold, W. Gu, S. P. Cramer and C. G. Riordan, *J. Am. Chem. Soc.*, 2001, **123**, 9194.

24 (*a*) M. S. Bharara, S. Parkin and D. A. Atwood, *Inorg. Chem.*, 2006, **45**, 2112; (*b*) M. S. Bharara, T. H. Bui, S. Parkin and D. A. Atwood, *Dalton Trans.*, 2005, 3874.

25 (*a*) A. Bondi, *J. Phys. Chem.*, 1964, **68**, 441; (*b*) D. Gredenic, *Quart. Rev. Chem. Soc.*, 1965, 303; (*c*) A. J. Canty and G. B. Deacon, *Inorg. Chim. Acta*, 1980, L225; (*d*) J. L. Wardell, *Organometallic Compounds of Zinc, Cadmium and Mercury*, Chapman and Hall, 1985, pp. 11–129.

26 L. Yang, D. R. Powell and R. P. Houser, *Dalton Trans.*, 2007, 955.

27 Y. Liu, F. Wei, S. N. Yeo, F. M. Lee, C. Kloc, Q. Yan, H. H. Hng, J. Ma and Q. Zhang, *Inorg. Chem.*, 2012, **51**, 4414.

28 A. W. M. Lee, W. H. Chan and H. C. Wong, *Synth. Commun.*, 1988, **18**, 1531.

29 Oxford Diffraction, CrysAlis CCD, RED, version 1.711.13, copyright (1995–2003), Oxford Diffraction Poland Sp.

30 G. M. Sheldrick, *SHELXS97, Program for Crystal Structure Solution*, University of Gottingen, Gottingen, 1997.

31 G. M. Sheldrick, *SHELXL97, Program for Crystal Structure Refinement*, University of Gottingen, Gottingen, 1997.

32 M. N. Burnett and C. K. Johnson, ORTEP-III, Oak Ridge Thermal Ellipsoid Plot Program for Crystal Structure Illustrations, Report ORNL-6895, Oak Ridge National Laboratory, Oak Ridge, TN, USA, 1996.

33 Mercury CSD 2.0 – New Features for the Visualization and Investigation of Crystal Structures; C. F. Macrae, I. J. Bruno, J. A. Chisholm, P. R. Edgington, P. McCabe, E. Pidcock, L. Rodriguez-Monge, R. Taylor, J. van de Streek and P. A. Wood, *J. Appl. Crystallogr.*, 2008, **41**, 466–470, DOI: 10.1107/S0021889807067908.

34 R. Dennington, T. Keith and J. Millam, *GaussView, Version 5*, Semichem Inc., Shawnee Mission, KS, 2009.

35 M. J. Frisch, G. W. Trucks, H. B. Schlegel, G. E. Scuseria, M. A. Robb, J. R. Cheeseman, G. Scalmani, V. Barone, B. Mennucci, G. A. Petersson, H. Nakatsuji, M. Caricato, X. Li, H. P. Hratchian, A. F. Izmaylov, J. Bloino, G. Zheng, J. L. Sonnenberg, M. Hada, M. Ehara, K. Toyota, R. Fukuda, J. Hasegawa, M. Ishida, T. Nakajima, Y. Honda, O. Kitao, H. Nakai, T. Vreven, J. A. Montgomery, J. E. Peralta Jr., F. Ogliaro, M. Bearpark, J. J. Heyd, E. Brothers, K. N. Kudin, V. N. Staroverov, R. Kobayashi, J. Normand, K. Raghavachari, A. Rendell, J. C. Burant, S. S. Iyengar, J. Tomasi, M. Cossi, N. Rega, J. M. Millam, M. Klene, J. E. Knox, J. B. Cross, V. Bakken, C. Adamo, J. Jaramillo, R. Gomperts, R. E. Stratmann, O. Yazyev, A. J. Austin, R. Cammi, C. Pomelli, J. Ochterski, R. L. Martin, K. Morokuma, V. G. Zakrzewski, G. A. Voth, P. Salvador, J. J. Dannenberg, S. Dapprich, A. D. Daniels, O. Farkas, J. B. Foresman, J. V. Ortiz, J. Cioslowski and D. J. Fox, *GAUSSIAN 09 (Revision A.2)*, Gaussian, Inc., Wallingford, CT, 2009.